MOUNTAIN-PLAINS CONSORTIUM

MPC 24-569 | W. Davis and P. Heyliger

MONITORING TRANSPORTATION STRUCTURE INTEGRITY LOSS AND RISK WITH STRUCTURE-FROM-MOTION

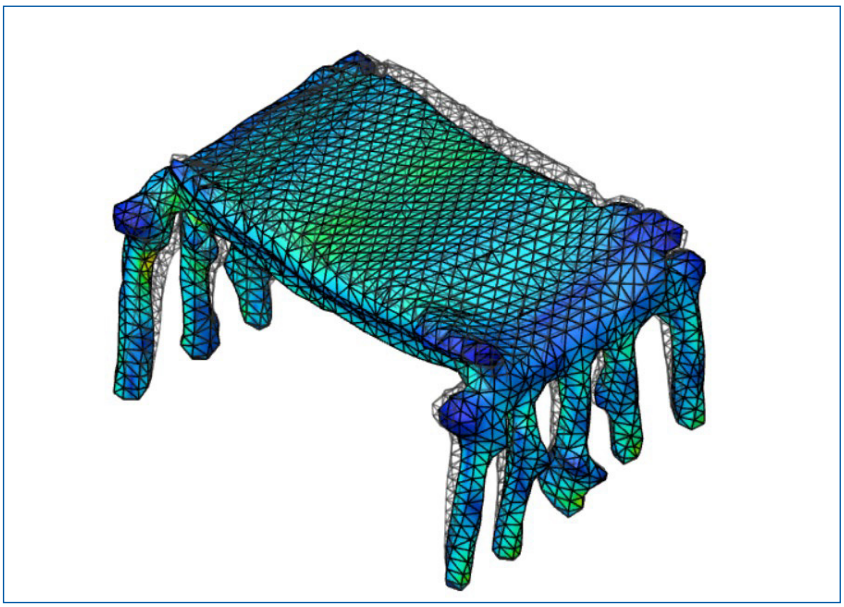

MOUNTAIN-PLAINS CONSORTIUM REGION 8

A University Transportation Center sponsored by the U.S. Department of Transportation serving the Mountain-Plains Region. Consortium members:

Colorado State University
North Dakota State University
South Dakota State University
University of Colorado Denver
University of Denver
University of Utah
Utah State University
University of Wyoming

Technical Report Documentation Page

1. Report No.	2. Government Accession No.	3. Recipient's Catalog No.
MPC-571		

4. Title and Subtitle	5. Report Date
Monitoring Transportation Structure Integrity Loss and Risk with Structure-From-Motion	August 2024
	6. Performing Organization Code

7. Author(s)	8. Performing Organization Report No.
Will Davis Paul Heyliger	MPC 24-569

9. Performing Organization Name and Address	10. Work Unit No. (TRAIS)
Department of Civil and Environmental Engineering Colorado State University Fort Collins CO 80523	11. Contract or Grant No.

12. Sponsoring Agency Name and Address	13. Type of Report and Period Covered
Mountain-Plains Consortium North Dakota State University PO Box 6050, Fargo, ND 58108	Final Report
	14. Sponsoring Agency Code

15. Supplementary Notes

Supported by a grant from the US DOT, University Transportation Centers Program

16. Abstract

This report describes methods that allow for assessing structural integrity using a direct porting of imaging methods captured by both hand-held and uncrewed aircraft system (UAS)-assisted photography into computational analysis tools to monitor structural degradation of transportation structures. Of primary interest is the level of accuracy of cracked structures and their evolution over time using structure from motion (SfM). Imaging methods using light detection and ranging (LidDAR scanning, and the modeling of particle flow are also explored, with the focus of these two techniques being longer, more slender structures and the effects of debris flow on transportation infrastructure. Imaging techniques show great promise, with cracks being detected down to the centimeter scale, while finite element and discrete element models also show potential in these image-to-model simulations.

17. Key Word	18. Distribution Statement
finite element method, methodology, photographs, structural health monitoring	Public distribution

19. Security Classif. (of this report)	20. Security Classif. (of this page)	21. No. of Pages	22. Price
Unclassified	Unclassified	28	n/a

Form DOT F 1700.7 (8-72) Reproduction of completed page authorized

Monitoring Transportation Structure Integrity Loss and Risk with Structure-From-Motion

Will Davis
Paul Heyliger

Department of Civil and Environmental Engineering
Colorado State University
Fort Collins CO 80523
prh@engr.colostate.edu

October 2024

Disclaimer

The contents of this report reflect the views of the authors, who are responsible for the facts and the accuracy of the information presented. This document is disseminated under the sponsorship of the Department of Transportation, University Transportation Centers Program, in the interest of information exchange. The U.S. Government assumes no liability for the contents or use thereof.

ABSTRACT

This report describes methods that allow for assessing structural integrity using a direct porting of imaging methods captured by both hand-held and uncrewed aircraft system (UAS)-assisted photography into computational analysis tools to monitor structural degradation of transportation structures. Of primary interest is the level of accuracy of cracked structures and their evolution over time using structure from motion (SfM). Imaging methods using light detection and ranging (LidDAR scanning, and the modeling of particle flow are also explored, with the focus of these two techniques being longer, more slender structures and the effects of debris flow on transportation infrastructure. Imaging techniques show great promise, with cracks being detected down to the centimeter scale, while finite element and discrete element models also show potential in these image-to-model simulations.

TABLE OF CONTENTS

LIST OF FIGURES

1. INTRODUCTION

U.S. transportation infrastructure faces at least two main challenges: age and usage. Despite heavy investments in maintenance, repair, and upkeep, managing these challenges with limited financial resources will always require triage and a constant supply of updated and accurate inspection data provided by a variety of methods. Despite significant efforts, dramatic improvements in technology, and a variety of inspection guidelines, current inspection methods have sometimes proved inadequate. Figure 1.1 shows two railway line failures, including one incident where the tracks had been inspected multiple times in the weeks prior to the accident, including one completed the same day as the accident. Part of the challenge comes down to labor and resources.

Figure 1.1 Two significant derailment failures: Left: 30 BNSF rail cars hauling coal near Pueblo, Colorado, derailed on October 15, 2023, causing extensive damage and one death on I-25 below the bridge (photo courtesy of KVDR); right: 16 rail cars, 15 of which had hazardous material, derailed on June 24, 2023, at Reed Point, Stillwater County, Montana (photo NTSB). In the former case, the tracks had been inspected on the day of the accident.

Professor Allan Zarembski of the University of Delaware has noted that "the track has to be walked, physically walked, or inspected at a very low speed from a slow-moving vehicle once or twice a week depending on the criteria." Regarding another rail accident, the National Transportation Safety Board (NTSB) stated, "We also found that walking inspections are important to ensure an understanding of track conditions and that the track inspector's workload likely prevented him from performing a timely walking inspection of the track in the area of the derailment" (NTSB 2023). Hence there is a huge need to potentially accelerate the inspection process or, at a minimum, develop inspection tools that provide workers with more efficient resources.

One of these methods involves a class of imaging tools that can rapidly and objectively track and assess levels of cracking or damage. Generally known as photogrammetric methods, these techniques use a series of conventional photographic images to create a point cloud that can then be translated to a three-dimensional image. These methods have seen extensive application and use in a wide variety of fields. One extension of this method is to use the point cloud data to re-create a three-dimensional image that can be modeled using conventional structural analysis tools such as the finite element method (FEM) or the discrete element method (DEM).

In general, these images can most accurately be captured by hand-held cameras used by inspection personnel. However, in the past decade, one new method class has the potential to assist in the accelerated and possibly more accurate inspection process, which includes using uncrewed aircraft systems (UASs). These systems provide a great deal of flexibility, efficiency, and mobility that can be exploited to potentially revolutionize how, and in what level of detail, transportation infrastructure can be inspected (Whitehead and Hugenholtz 2014). This is especially true for bridges (Chan et al. 2015, Ellenberg et al. 2016, Dorafshan et al. 2017, 2018), where the maneuverability of UAS aircraft have proven to have significant potential. UAS tools have also shown great promise in evaluating both paved (All Sourav et al. 2023) and unpaved surfaces (Zhang and Elaksher 2012).

This study reports on several attempts to unite many of these photogrammetry and analysis tools to simulate some of the more prevalent areas of damage. To reduce the scope of the work to something reasonable, the focus was on two areas: 1) the level of cracking and surface damage that can be captured from imaging methods, and 2) the modeling of one type of natural hazard that can cause considerable damage: particle flow. This is especially timely in areas following post-fire runoff zones that can experience significant erosion or damage to bridges, culverts, and retaining walls because of the dynamic loads of larger particles on the supporting structure.

2. PHOTOGRAMMETRY FOR FINITE ELEMENT MESH STRESS ANALYSIS

This chapter describes the primary imaging method along with its combination with finite element analysis tools for several test objects.

Photogrammetry is a modern-day tool that enables users to model an object or structure without taking the time and effort necessary to make an accurate computer aided design (CAD) drawing and convert the drawing to a finite element mesh. The goal of this phase of the work is to find a way to take a photogrammetry scan of a structure and convert it to a three-dimensional finite element model for subsequent stress analysis. The benefits of this stress analysis process are its simplicity, its affordability, and the small amount of time required by the user to make a stress simulation.

Test Case: The Stump

To start this project, tests were performed on small or simple objects to evaluate whether or not photogrammetry was a feasible option for broader application. For a variety of reasons, including the safety of the photographer around transportation structures, the first object used for these tests was a cracked tree stump, as shown below in Figure 2.1.

Figure 2.1 An image of a tree stump used for imaging and inspection models. This structure was selected because of the wide variety of crack shape and size, the large amount of surface change over the object, the fact that the cracks change size over time as the moisture concentration changes, and the safety of the imaging environment.

Photogrammetry works by taking a series of photos of an object and converting the photos into a model of the object. In this initial application, photos were taken of all sides of the stump by varying the height and angle of orientation of the lens. The number of photos taken was determined by the size and complexity of this item, with 51 photos taken in this case. This number is relatively small but was used because the lighting was ideal and the object being modeled was not very large. The quality of the photos taken of this stump played a crucial role in obtaining an accurate 3D model. Initially, a cell phone camera was used to capture the images.

However, the resolution obtained was poor. Far better images were obtained using a Nikon D90 camera, which was then used for all for subsequent test models. The lighting on the object was critical because if a shadow was cast on any part of the object, that piece would not appear in the fully rendered model.

The photos of the stump were taken on an overcast day, which provided even lighting to achieve the best results. After the photos were taken, they were uploaded to and processed in Agisoft MetaShape, a photogrammetry software package. A planar image generated by MetaShape is shown in Figure 2.2, but it is important to note that this is just a single view of a three-dimensional object that can be viewed from any angle or height.

Figure 2.2 A planar image of the rendering of the result of photogrammetry imaging of 51 planar still photos of the cracked stump.

After the photos were taken of this stump, the MetaShape software was used to convert the photos into a 3D model in the form of an STL (standard tessellation language) filetype. The STL project file was then imported in the meshing software MeshMixer (made by AutoDesk) to downsize and repair the STL file so it could be imported into 3D CAD software. Figure 2.3 shows a photo of the model after being downsized and repaired in MeshMixer in the form of an STL.

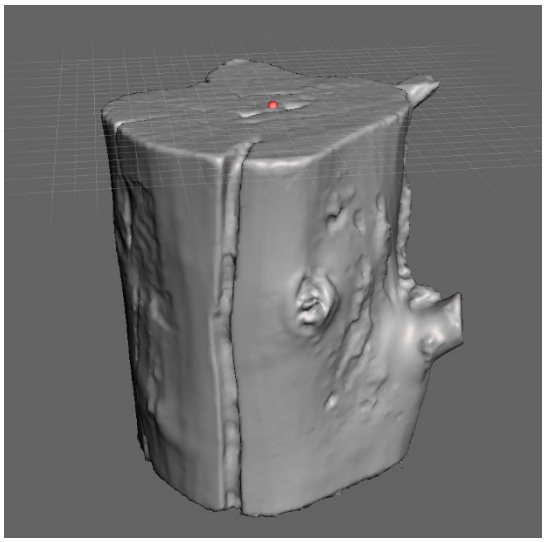

Figure 2.3 The results of the STL file conversion from the rendered stump image so that it can be transferred into an AutoCad file for meshing and analysis.

The resulting STL file was then exported from MeshMixer to AutoDesk Fusion360 for orientation and scaling and to create a mesh that can be exported into finite element analysis software. A photo of the scaled and oriented mesh is shown in Figure 2.4.

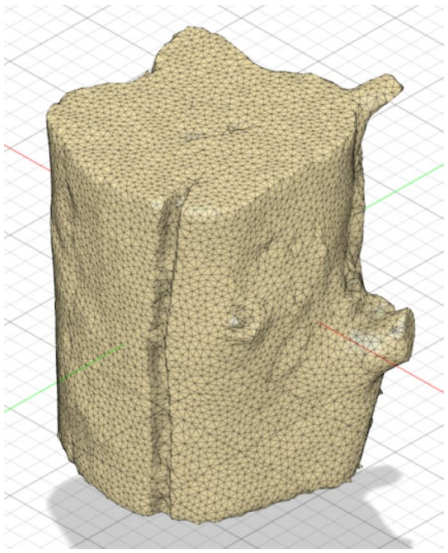

Figure 2.4 The three-dimensional finite element mesh after the CAD file has been converted to a three-dimensional elastic solid. This mesh can then be used for subsequent analysis. This is an extremely fine mesh that would most likely be excessive for preliminary analysis and require extensive computational time.

Because of the low computation power of the computer used, this original finite element model was downsized using the Fusion360 “remesh” feature so that the mesh had fewer than 10,000 faces and did not have any elements overlapping each other. This resulted in a significant drop in subsequent computational time. Figure 2.5 shows a photo of the reduced mesh.

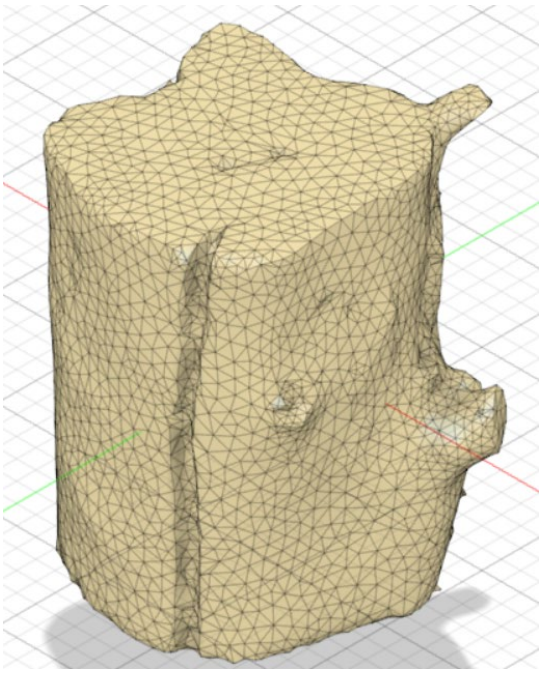

Figure 2.5 A coarser mesh of the stump used in Figure 2.4. This maintains the geometry but results in a far more efficient structural analysis.

After the model was re-meshed, the conversion tool in Fusion360 was used to convert the STL mesh to a STEP mesh so that it could be imported into FEM analysis software. Figure 2.6 shows a photo of the final 3D CAD file used in the final mechanics analysis.

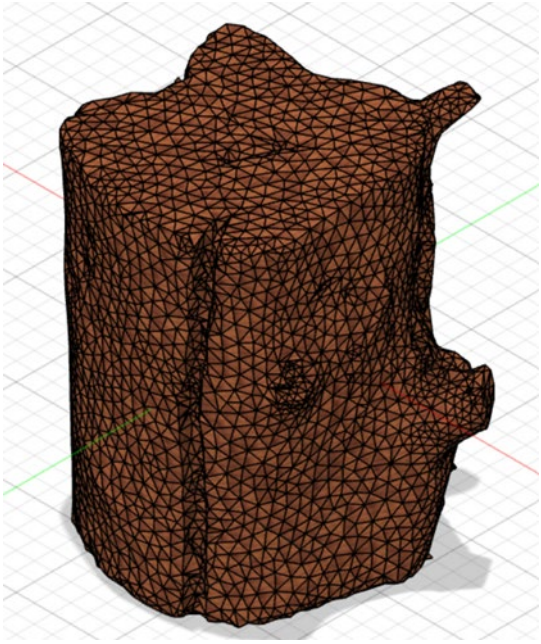

Figure 2.6 The final finite element mesh used to complete a three-dimensional stress analysis. This is an example used to demonstrate the imaging to model sequence, and the actual results of this analysis were of little practical value. However, crack tip elements and other features of fracture mechanics could easily be introduced into this model.

Several comments are in order that influence the choice of finite element modeling routines that can be used in a conventional analysis environment, and these decisions will obviously be influenced by the institution's computational assets. Here we describe one sequence using the resources available at the author's institution. After converting the model to a STEP file, the object's properties were used to determine which FEM analysis software would be used to simulate a load on the object. If the model was simple and composed of an isotropic material, Fusion360's built-in stress simulation software was used for the stress analysis simulation. If the model was complex, composed of multiple materials, or made of a non-isotropic material, AutoDesk Inventor Nastran was used. Fusion360 Simulation and Inventor Nastran both use Nastran code for the simulations so there is little difference in the accuracy achieved or choices available to represent the model.

For this specific test case, Fusion360's built-in Nastran code simulation software was used to perform a complete stress analysis. The first step of Fusion360's simulation process is to choose a material that is as close to the object's actual material as possible, and this will depend on the specific material being studied (here it was white oak). The next step is to set a virtual constraint on the object in the stress analysis software where the object is physically restrained by the ground, a bolt, or another physical restraint. After the constraints are in place, loadings are placed on the model using the software wherever the desired location for the load simulation is on the physical structure. The Nastran Code Solver is then used to solve the stress simulation. The finished product is used to determine the needed information about stress and displacement fields, areas of stress concentration, or displacement patterns. Figure 2.7 shows a photo of the von Mises contours for this stump under a uniform upper surface load.

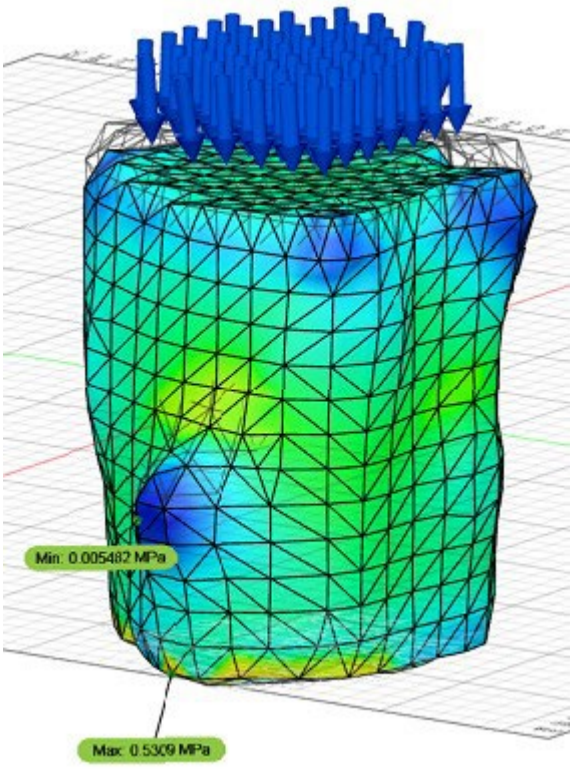

Figure 2.7 von Mises stress contours for a typical loading of the stump, where the bottom surface was fixed, and a uniform vertical stress is applied to the upper surface.

Application Case: The Railroad Bridge

The next more complex structure chosen for applying this methodology was an old, rotting railroad bridge in north Fort Collins. This bridge is no longer in use but was once capable of bearing a tremendous amount of weight. A very similar process was used to model and analyze this structure as was used for the stump. To start, a series of photos was taken of all sides of the bridge. A total of 71 photos were taken of the bridge. These photos were then processed with MetaShape to form a 3D model in the form of an STL. A photo of the 3D model is shown in Figure 2.8.

Figure 2.8 Final SfM image of railroad bridge in northern Fort Collins. This is a two-dimensional capture of the full three-dimensional model that can be viewed from any angle or orientation/height.

MeshMixer was then used to mesh the bridge and to resize and repair the mesh so that it could be imported into Fusion360. MeshMixer was also used to fill any "holes" in the model that would prevent it from being used for finite element analysis. Fusion360 was then used to further refine the model and to size the mesh to the desired saturation. We eliminate a detailed explanation of the entire process since these steps replicate what was accomplished for the introductory test case using the wooden stump. Figure 2.9 shows a photo of the completed mesh from Fusion360.

Figure 2.9 The final three-dimensional finite element mesh of the rail bridge following several intermediate steps moving from images to final numerical model.

This mesh was then used in the same simulation process that the stump model was run through but with a load simulating a train on the top of the bridge. The necessary mesh refinement required a relatively large number of elements to run, but there were no other computational issues. A picture of the simulation is shown in Figure 2.10.

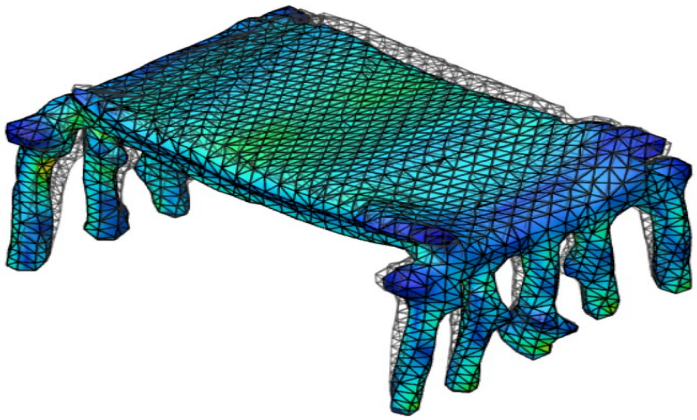

Figure 2.10 The von Mises stress contours for the rail bridge with a load simulating gravity loads from a rail car.

Additional Application: A Historic Barn

A final test was performed on a historic barn located in Northern Colorado. This structure was selected because it had significant signs of cracks and decay, but it resembled a traditional building of four walls and a roof, as seen in Figure 2.11. This structure is able to withstand high velocity wind without issues even in its current condition.

Figure 2.11 A historic barn structure used to examine the accuracy of the SfM methodology for a relatively simple geometry.

A total of 126 photos were taken of all sides of the barn. These photos were then converted into a 3D STL model with the software MetaShape. This test provided some of the most visually appealing results yet because the structure is very simple and has flat, symmetric sides without much complex geometry. Figure 2.12 shows the three-dimensional model of the barn in MetaShape following processing of the point cloud.

Figure 2.12 A still shot of the rendered image from SfM software with excellent resolution for a relatively small number of still images.

As before, some details of the process are omitted here since they are the same steps as used for the earlier structures. After the model was finished being processed in MetaShape, MeshMixer was used to mesh the barn model and fill in any holes in the model. MeshMixer was also used to scale the mesh to a size that a CAD software could import. Fusion360 was then used to size the mesh to the desired saturation and to convert the model from an STL to a STEP file so that a finite element analysis could be performed. The model following the STEP file is shown in Figure 2.13.

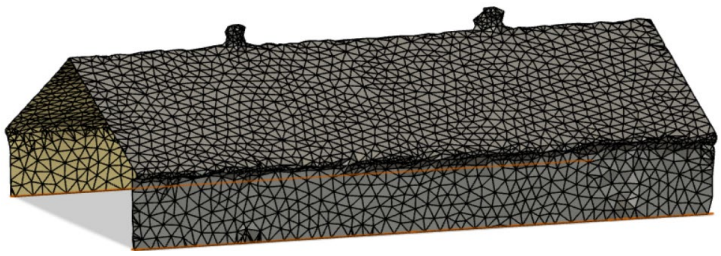

Figure 2.13 The STEP file used at the front end of the finite element analysis.

As a final step, the built-in Nastran solver in Fusion360 was used to put a simulated wind load on one side of the barn. The load was placed on the west side of the barn because the wind generally comes from this direction. Figure 2.14 shows a photo of representative results.

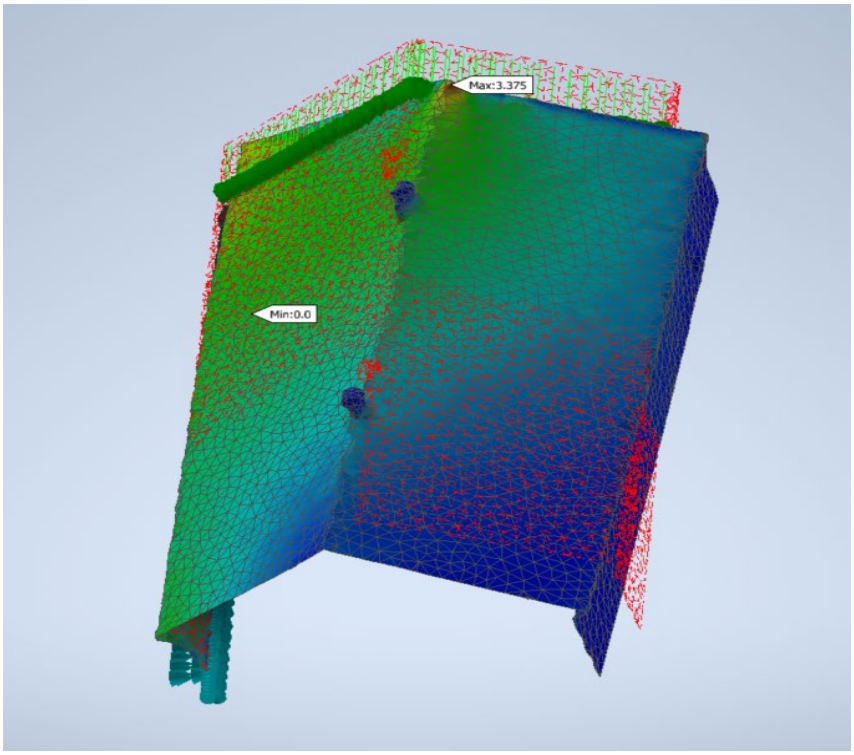

Figure 2.14 Typical results from a stress analysis of the historic barn structure.

Low-End Lidar Applications: Widar

To explore options other than a traditional photogrammetry software for creating models for finite element analysis, a series of android applications were also tested as part of this research to see if they would create a model that was sufficiently accurate. The applications tested were PolyCam, Widar, and Kiri engine. Of these applications, Widar was the only cost-free option, and it proved to be the best application for the intended use of this project.

To make a model using Widar, a series of photos are taken through a phone app. These are then uploaded to a server that converts them into a model. The server only takes a few minutes to complete an entire model. This method of making 3D models is very useful when a high-speed modeling technique is needed. Using this technique sacrifices some accuracy as a result of the fast computation time, but there are some benefits to this imaging tool. A photo of a Widar-generated model of the stump used for the first photogrammetry test is shown in Figure 2.15.

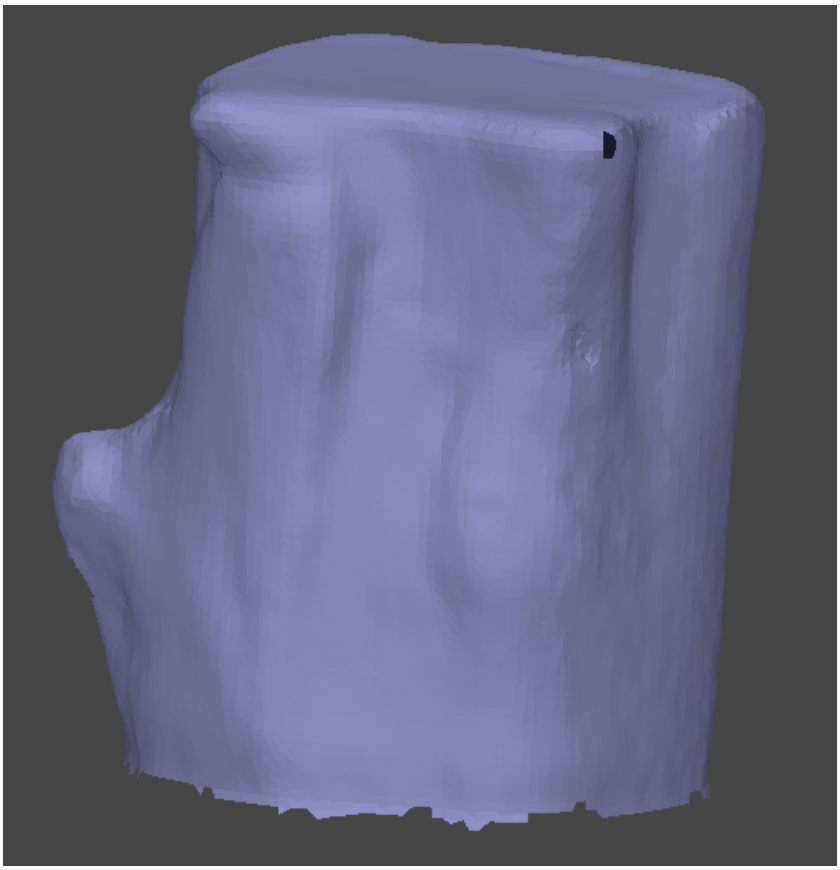

Figure 2.15 A Widar-generated model of the same stump used in SfM.

This model was then imported directly to Fusion360 for stress analysis. Figure 2.16 shows a photo of the model and the resulting stress contours.

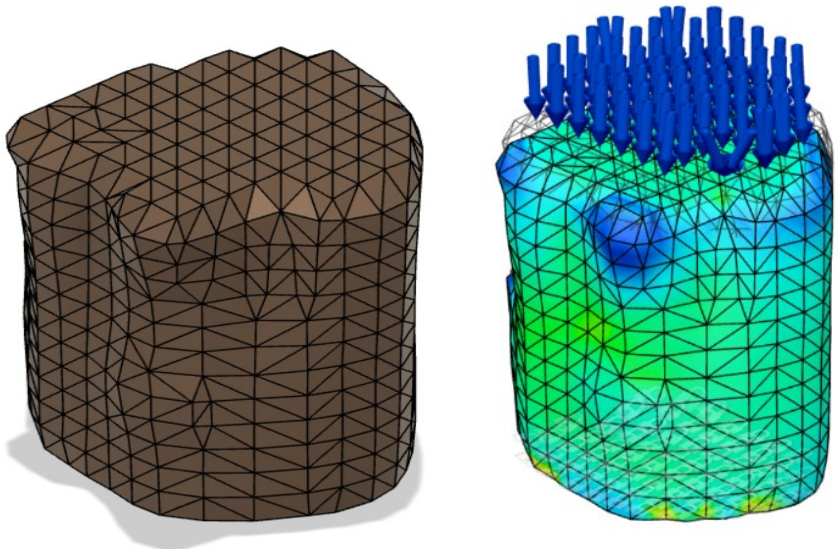

Figure 2.16 A Widar-generated finite element mesh (left) and the resulting stress contours (right) for a uniform vertical load. The results are extremely close to those developed by SfM.

This model is much coarser than the photogrammetry model because of the application's limitations. However, this method is still very accurate for structures with simple geometries and when high levels of accuracy are not needed.

We explored several other comparisons of structural representations when using SfM versus Lidar/Widar applications. Figure 2.17 shows the walls of the historic Fort Vasquez in Colorado. As a second example, we also imaged a raptor nest from Staunton State Park in Colorado using both Lidar and SfM methods. The results are shown in Figure 2.18.

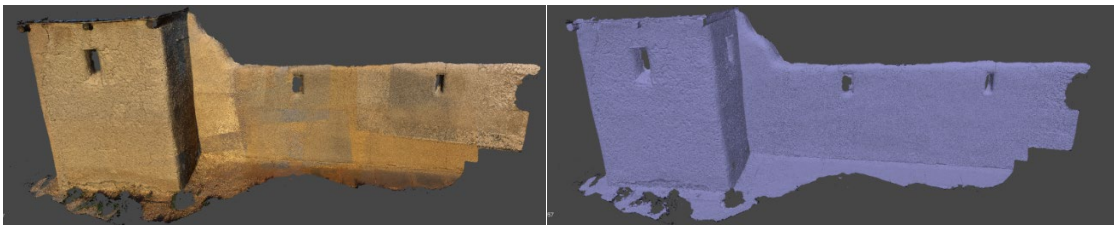

Figure 2.17 Lidar (left) and SfM (right) generated images of a severely weathered exterior wall of the historic Fort Vasquez in northern Colorado. Both methods capture larger voids and cracks. Lidar-based methods are faster but less accurate than SfM models, in general.

Figure 2.18 SfM (left) and Lidar (right) based models of a raptor nest in Staunton State Park in Colorado.

Although these specific structures are not transportation-related, they possess many of the same characteristics of the types of environmental degradation that can be found in these systems. These results show the potential that photogrammetry methods can deliver.

3. TRACKING AND MODELING PARTICLE FLOW

One type of application for which photogrammetry can eventually be applied is in tracking the process of natural hazards, including rockfall or movement of granular media. An example, seen in Figure 3.1, is a recent rockfall on Highway 14 in Colorado, where several large boulders collided with the pavement below.

Figure 3.1 Rockfall damage on Highway 14 on June 9, 2023, at 6 AM. The PI and colleagues (right) were on scene to investigate the level of damage and attempt to image the resulting starting and final position of the rockfall. The highway was closed for about four hours, but after an incredible response by CDOT was shortly reopened despite significant damage to the surrounding asphalt.

This phase of the research consisted of developing a discrete element model (DEM) to track the flow of particles of varying size. The intent of this work is to be able to understand the physics of particle flow by tracking the positions of each particle as they deform. In addition to the rockfall situation shown in Figure 20, another example of this type of problem is shown in Figure 3.2. This is a typical scenario following fire damage: a huge amount of erosion and aggregate flow in a formerly pristine stream.

Figure 3.2 Remediation efforts in the Saint Vrain River following wildfire damage, November 21, 2017. Bales of hay and other natural fibrous materials are being used as reinforcement along the riverbank.

Discrete Element Modeling of Particle Flow

This phase of the research involved the development of a new discrete element model to model and track the flow of particles via numerical simulations. This part of the research has been completed and was published as a journal article (Jiang, C., Bareither, C., and Heyliger, P.R. "Confined Binary Particle Mixing with a Modified Discrete Element Method," *Computational Particle Mechanics*, May 2024). Rather than repeat the content of that document, we highlight several key features below.

Figure 3.3 shows the dominant effect of the new DEM model: the complex relationship between sticking and slipping contact between two particles. This behavior is very difficult to capture numerically and involves a constant updating of the contact conditions between the surfaces of the two particles. As the analysis steps through time, the contact conditions must be continuously updated to see if there is sticking, sliding, or no contact. The resulting forces acting on the particle are then updated and the analysis proceeds.

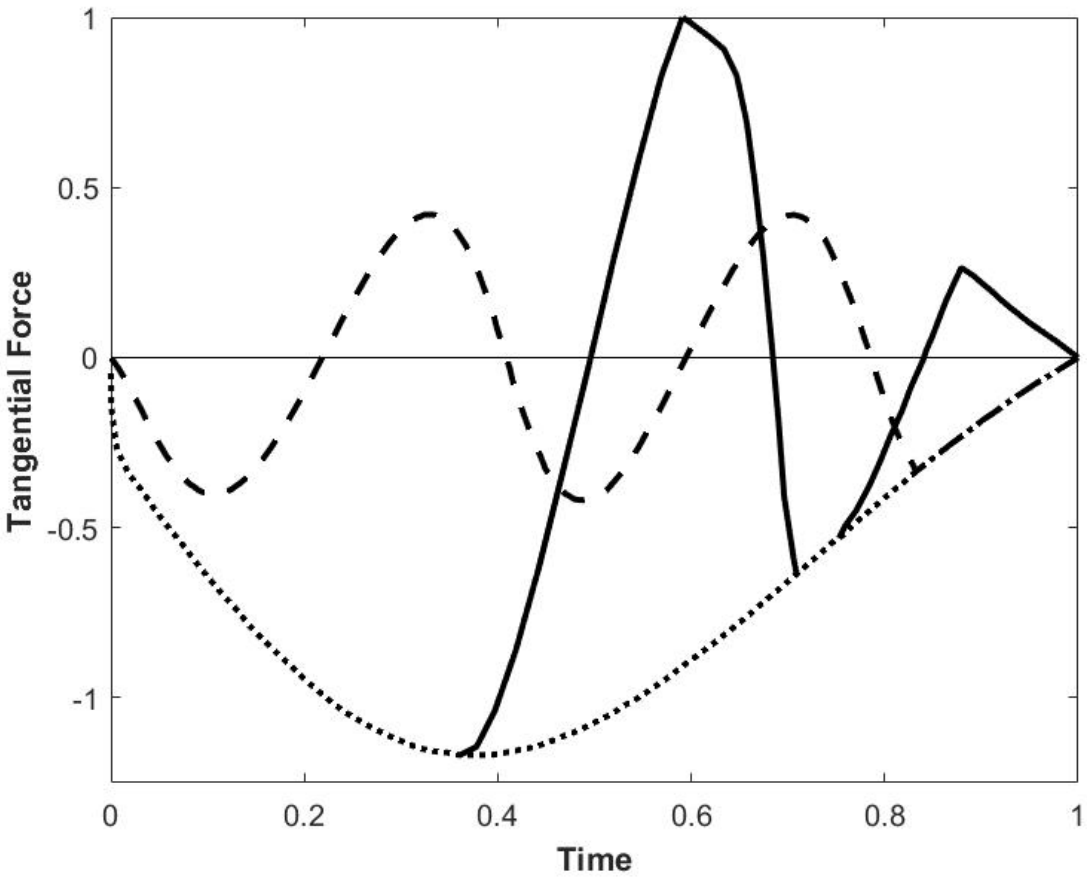

Figure 3.3 Evolution of tangential forces on spheres during impact with varying angles using the developed DEM model and input parameters from impact between a sphere and a rigid wall. The dashed line shows the force for a sphere with a relatively small radius of gyration and a small angle of incidence. The dotted line is the tangential force for a sphere that has a high angle of incidence and is in gross slip during the entire contact. The solid line is for a sphere with an intermediate angle of incidence that transitions between stick and slip during the compression/restitution phase of contact.

To determine the accuracy of the model, there are a widely used set of benchmark studies that use more detailed analyses than those usually contained in DEM models. In this study, we compared our new DEM model with these results. Overall, the new DEM model was at a minimum as good as, if not better than, existing DEM models. A representative plot in Figure 3.4 shows how the benchmark results of a sphere with constant angular velocity and varying tangential velocities is impacting a rigid plane. Here the new DEM model clearly gives better agreement with the finite element results of Wu than other DEM results.

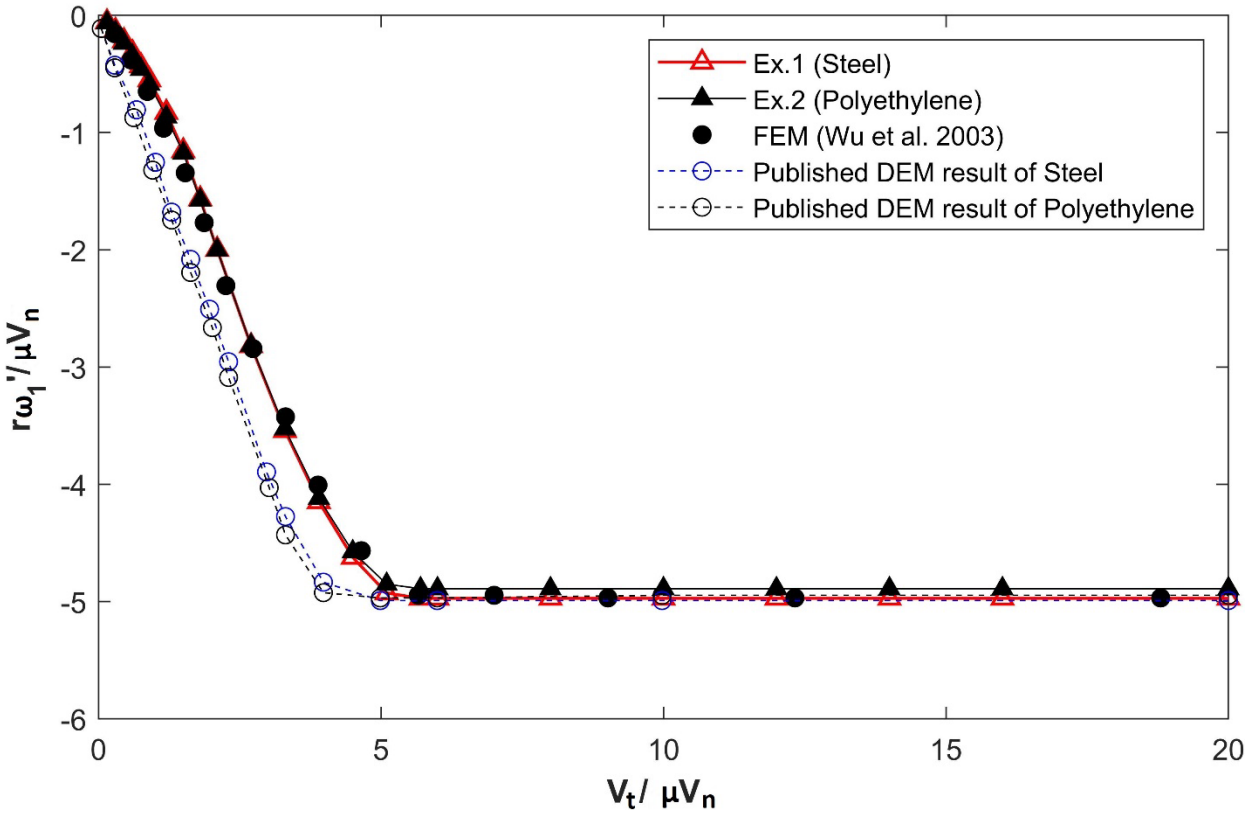

Figure 3.4 Results from a standard benchmark test of particle collisions. These show how the present model (solid dark triangles) are in far better agreement with standard finite element results (solid circles) than those of a more simplified DEM model (hollow circles).

Finally, we simulate particle flow by mixing particle groups of varying size past geometric mixers, as shown in Figure 3.5. This is an extremely complex problem for which there are no existing results. However, the qualitative results of this work showed very good agreement with large-scale field tests that have been completed by other workers.

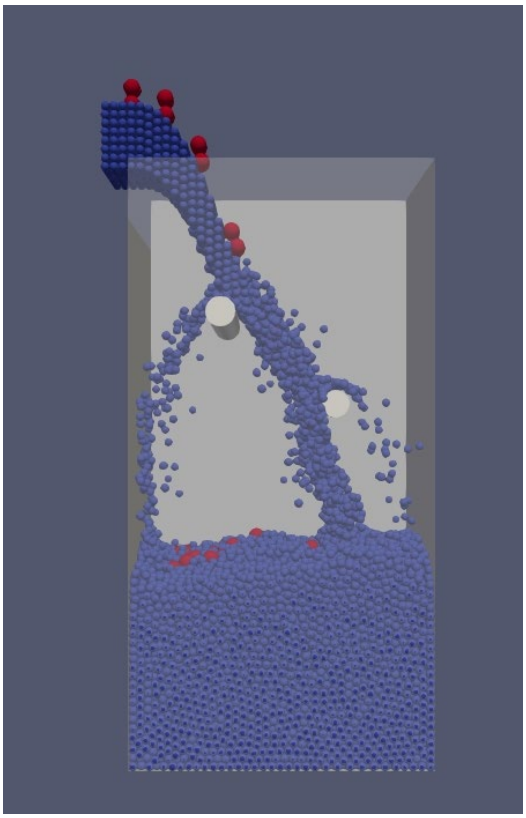

Figure 3.5 A still photo from a video simulation of binary particle collisions directed by two barriers. This class of problem was explored by a newly developed DEM model that can explicitly model this type of granular interaction.

4. SUMMARY AND CONCLUSIONS

Several photogrammetry methods, including structure-from-motion and Lidar, were applied to studying representative problems to introduce a methodology for studying damage and structural integrity loss. In addition, we attempted to apply this methodology to a common natural hazard for transportation infrastructure: the flow of particles/rocks/aggregate during flood or post-fire erosion.

Our key findings included the following:

1. Cracks in buildings and roadways can be identified well below a distance 1 cm and frequently far below this.
2. We have developed and applied a methodology for performing a complete structural analysis moving from digital images, acquired from either hand-held cameras or uncrewed aircraft systems, through several image processing schemes, into a finite element analysis of representative structures.
3. We developed a discrete-element model to represent the interacting particles that simulate particle flow during flood or rockfall events. This new approach provided excellent agreement with existing numerical models and can be used to further extend our methodology for very difficult to capture particle movement.